Environmental Pollution 341 (2024) 122911

Contents lists available at ScienceDirect

Environmental Pollution

journal homepage: www.elsevier.com/locate/envpol

Catalytic torrefaction effect on waste wood boards for sustainable biochar production and environmental remediation☆

Larissa Richa [a], Baptiste Colin [a], Anélie Pétrissans [a], Jasmine Wolfgram [b], Ciera Wallace [b], Rafael L. Quirino [b], Wei-Hsin Chen [c,d,e,*], Mathieu Pétrissans [a]

[a] Université de Lorraine, INRAE, LERMaB, F-88000, Epinal, France
[b] Chemistry Department, Georgia Southern University, Statesboro, GA-30460, USA
[c] Department of Aeronautics and Astronautics, National Cheng Kung University, Tainan, 701, Taiwan
[d] Research Center for Smart Sustainable Circular Economy, Tunghai University, Taichung, 407, Taiwan
[e] Department of Mechanical Engineering, National Chin-Yi University of Technology, Taichung, 411, Taiwan

ARTICLE INFO

Keywords:
Waste wood board
Potassium
Torrefaction
Pyrolysis
Regression analysis
Exothermic reactions

ABSTRACT

Wood boards used in construction are generally treated with toxic chemicals, making them unsuitable for further use and causing environmental pollution. This study evaluates the possibility of using catalytic torrefaction as a pretreatment to improve wood pyrolysis and combustion for greener biochar production. Waste beech boards were impregnated with different K_2CO_3 solutions (0–0.012 M), then torrefied between 5 and 60 min at 275 °C. The ICP-AES showed that the board's surface held more potassium than the core. Torrefaction coupled with potassium decreased the C–O and –OH stretches. Thermogravimetric analysis of torrefied wood showed that the board's internal heating degraded the core more than the surface. The exothermic reactions made potassium's catalytic action more efficient in the core. Interactions between the potassium content and torrefaction duration decreased the pyrolysis' maximum devolatilization temperature. During combustion, potassium decreased the ignition temperature by up to 9% and 3% at the surface and core, respectively, while the torrefaction increased it. The catalytic torrefaction significantly decreased the devolatilization peak during combustion, thus making the wood's combustion similar to that of coal, having only the char oxidation step. These findings highlight the advantages and challenges of waste wood's catalytic-torrefaction for biochar production to reduce environmental pollution.

1. Introduction

Torrefaction, known as mild pyrolysis, has been established as an effective pretreatment method to upgrade biomass properties for energy production. It is a thermochemical conversion process that operates under 200–300 °C in an inert atmosphere (Silveira et al., 2021a). Depending on the torrefaction or pyrolysis conditions, the reaction heat can either be endothermic or exothermic (Bates and Ghoniem, 2013). This shift could depend on the competition between exothermic reactions (char formation) and endothermic reactions (volatiles formation) (Rath, 2003). Torrefaction could be used as an alternative to toxic processing methods to improve wood's durability (i.e., chromated copper arsenate treatment used for construction wood) (Robey et al., 2018). When studying torrefaction's impact on the waste wood, it improves the higher heating value by relatively increasing the carbon content and decreasing the volatile matter content (Chen et al., 2021a). This makes torrefaction a suitable solution for valorizing waste lignocellulosic biomass for energy production. Singh et al. (2020) reported a decrease of more than half of the pyrolysis' activation energy using torrefied wood compared to the raw. Torrefaction also increases the homogeneity of the biomass while making it more resistant to biological degradation, thus improving storage stability (Medic et al., 2012).

Aniza et al. (2023) and Kota et al. (2022) highlighted the importance of biowaste remediation through torrefaction to mitigate and reduce environmental pollution. Due to increasing environmental regulations, wood pellet torrefaction is being examined as a sustainable method for power generation and co-firing with coal (Kumar et al., 2017). Sher et al. (2020) state that co-firing torrefied beech with coal reduces SO_2 and NO_x emissions. Moreover, biomass co-firing could reduce combustion

☆ This paper has been recommended for acceptance by Rock Keey Liew.

* Corresponding author. Department of Aeronautics and Astronautics, National Cheng Kung University, Tainan, 701, Taiwan.
E-mail addresses: weihsinchen@gmail.com, chenwh@mail.ncku.edu.tw (W.-H. Chen).

https://doi.org/10.1016/j.envpol.2023.122911
Received 18 July 2023; Received in revised form 2 November 2023; Accepted 8 November 2023
Available online 13 November 2023

Nomenclature

Abbreviations

ICP-AES	Inductively coupled plasma atomic emission spectroscopy
FTIR	Fourier Transform Infrared
TGA	Thermogravimetric analysis
TG	Thermogravimetric curve
DTG	Derivative thermogravimetric curve
DTG_{max}	Maximum rate of DTG
db	Dry basis

Molecules

C	Carbon
O	Oxygen
H/H_2	Hydrogen/Dihydrogen
N/N_2	Nitrogen/Dinitrogen
K/K^+	Potassium/ion
K_2CO_3	Potassium carbonate
CO_2	Carbon dioxide
CO	Carbon monoxide
NO_x	Nitrogen oxide or Nitrogen dioxide
SO_2	Sulfur dioxide

Symbols

WL	Weight loss (wt% db)
T_{p1}	Pyrolysis peak temperature (°C) corresponding to local maximum rate of weight loss (DTG_{max1})
T_{p2}	Combustion peak temperature (°C) corresponding to the second local maximum rate of weight loss (DTG_{max2})
T_i	Ignition temperature (°C) calculated using the intersection method
T_b	Burnout temperature (°C) calculated using the intersection method

emissions by linking aluminum or sulfur silicates in coal with the alkali in biomass to form alkali silicate/sulfate that prevents the formation of corrosive compounds (Kassman et al., 2011). In addition, substituting coal with biomass significantly reduces the environment's organic carbon aerosols and CO_2 pollution (Li et al., 2021).

Catalytic torrefaction, more precisely using potassium as a catalyst, has been the subject of multiple studies (Macedo et al., 2022; Silveira et al., 2021a). Adding potassium to wood powder through impregnation reduces the torrefaction duration and the activation energy (Khazraie Shoulaifar et al., 2016). Moreover, potassium-impregnation of wood powder has been proven to inhibit levoglucosan production, a primary product of cellulose pyrolysis. Levoglucosan is a pollutant that remains in the atmosphere in the gas phase (i.e., in the clouds) or can condense on aerosol particles (Li et al., 2021). The pyrolysis of potassium-impregnated wood increases the gas yield, mainly H_2 and CO_2, and decreases tar production (Guo et al., 2016). Potassium-catalyzed pyrolysis accelerates the production of unsaturated aliphatic hydrocarbon and generates highly porous biochar that can be used as activated carbon (Shen et al., 2020). The biochar can assist recently-developed methods (i.e., carbon-based nanomaterials and nano zero-valent iron) in soil amendment and bio-adsorption (Lee et al., 2023; Li et al., 2023a, 2023b). K-rich biochars can improve crop productivity and reduce the leaching of valuable nutrients in the soil by increasing K availability, thus ensuring soil remediation (Widowati and Asnah, 2014). Potassium carbonate-activated biochar was highly efficient in adsorbing naphthalene, a highly toxic air pollutant (Zhu et al., 2018). Plus, activated carbon made from biochar was reported to have high adsorption of dyes such as crystal violet and methylene blue (Buhani et al., 2023; Elgarahy et al., 2023), and metals in water such as ferrous and manganous ions (Elwakeel et al., 2015). K-activated biochar also has high adsorption properties for lead, copper, sulfadiazine, and other pollutants (Yan et al., 2022; Zhang et al., 2020a). Operating at temperatures around 700 °C ensures that potassium remains in the biochar and poses no deposit formation or corrosion threat during pyrolysis or combustion (Zhang et al., 2020b). Recent studies show that increased potassium content in wood increases the exothermic reactions during packed-bed pyrolysis (Di Blasi et al., 2018).

However, until now, a wide range of studies has been limited to small wood particles varying between 0.05 and 0.5 mm (Chai et al., 2021; Zhang et al., 2019). Despite the scientific discoveries achieved by studying wood particles, it is not entirely representative of industrial conditions. Many studies highlight the importance of torrefying wood before grinding it and transporting it to be subsequently used for heat and power generation. These studies found that torrefying wood before grinding saves a substantial amount of energy required for the process, decreasing production costs (Chen et al., 2021a). Torrefied wood could be the key to pellet industrialization in the U.S.A. and European markets (Kumar et al., 2017). Furthermore, waste wood board torrefaction could reduce the reactor's volume required for this pretreatment compared to sawdust. The reactors used for waste wood board torrefaction are less complex and do not require particle-size reduction, meaning they are less expensive. Torrefying wood before transportation reduces the greenhouse gas emissions. This consequently lower the costs related to the increasing taxes on emissions (Kumar et al., 2017). Despite the significance of these findings, only a few torrefaction studies were performed on wood boards. Florez et al. (2023) reported an overshoot in the wood board's inner temperature that increases with the board's thickness. Perré et al. (2013) evaluated, using a dual-scale model, that stacking wood boards increases the exothermicity. Therefore, the few studies that focus on industrial-scale torrefaction emphasize the necessity of developing a more profound knowledge of wood board's torrefaction and, more precisely, catalytic torrefaction to properly assess the strengths and weaknesses of the process.

To the best of the authors' knowledge, torrefaction of waste wood boards with different potassium concentrations has never been done. Although it is recommended to torrefy wood boards before grinding to reduce energy consumption and CO_2 emissions extensively, no studies evaluate the feasibility of such a process. The work strategy combines the benefits of K-impregnation in facilitating the torrefaction pretreatment and producing highly adsorbant biochar that could be used for soil remediation. This paper aims to develop a deeper understanding of the K-impregnated waste wood's thermal degradation using wood boards with a thickness similar to the industry. The purpose is to evaluate the differences between the surface and the core of the board before and after torrefaction at 275 °C (5–60 min) with different potassium concentrations that were never addressed in the literature. Using Fourier-Transform Infrared (FTIR) spectroscopy, this work assesses the changes in the functional groups due to different torrefaction durations and potassium concentrations at the board's surface and core. The study digs further to evaluate the subsequent impact on pyrolysis and combustion of torrefied waste wood boards depending on the wood's potassium content by taking into consideration the board's thickness. In addition, the stability and reactivity of torrefied waste wood are evaluated during combustion. To the best of the authors' knowledge, no studies evaluate the influence of K on the pyrolysis or combustion of torrefied wood to produce biochar. The contribution of potassium to the exothermic reactions leading to a potentially self-heating process is assessed. This phenomenon has recently been discovered with very little knowledge, especially on a large scale. Consequently, this work sheds light on the benefits and challenges of waste wood boards' K-catalyzed

torrefaction for sustainable biochar production.

2. Materials and methods

2.1. Wood board preparation

Beech wood (*Fagus sylvatica*) was used in this study. It was acquired from the *Vosges PromoBois sawmill*, in Vosges region in France. The wood was issued from a larger board cut into 20 × 60 × 140 mm^3 board (radial × tangential × longitudinal directions following the wood fiber's orientation). The 20 mm thickness was chosen to match that of industrial-size boards. The boards were dried in an oven at 105 °C until mass stabilization to obtain the anhydrous weight of the samples.

The impregnation consisted of placing the dry wood in the impregnation tank (10 L capacity) and then filling it with the impregnating solution. It consisted of K_2CO_3 salt (Sigma Aldrich, 99.9% purity) mixed with deionized water for solutions with concentrations ranging from 0 (labeled washed) to 0.012 M with an increment of 0.004 M. The water-washing was done to obtain a basis for comparison with the impregnated samples, having undergone the same type of treatment. The impregnation was completed in two steps of 30 min each: a vacuum cycle at first at 110 mbar and a pressure cycle at 3 bars. The boards were allowed to dry at room temperature for 72 h before being placed in the oven at 105 °C until the weight stabilized. An additional sample for each K concentration was prepared (washed, raw, 0.004, 0.008, and 0.012 M). Some samples were used as control samples for measuring the K content in wood prior to torrefaction. The surface and core of the samples were extracted (Fig. S1) according to the procedure used in the literature (Florez et al., 2023). The surface represents the upper and lower part of the wood board in direct contact with the impregnation solution and the torrefaction atmosphere. The core represents the heart of the wood board to evaluate if the impregnation and torrefaction were similar between the core and the surface. The surface and core were ground each, and 200 mg were mineralized and passed to the atomic emission spectroscopy ICP-AES for minerals quantification throughout the wood board's thickness according to NF EN ISO 16967.

The wood boards were weighed before being placed in a sealed stainless-steel reactor. The atmosphere was kept inert using 100 mL·min^{-1} of N_2. The reactor was heated in a heating chamber where the temperature profile was controlled using a thermocouple. The samples were heated from room temperature to 275 °C using a heating rate of 2 °C·min^{-1}. The chosen temperature corresponds to a moderate torrefaction where enough differences in weight loss can be observed with potassium (Macedo et al., 2018). Then, they were kept at 275 °C for 4 different durations: 5, 15, 30, and 60 min. After cooling, the samples were removed, placed in a desiccator then weighed to obtain the final mass after torrefaction. The weight loss was obtained according to Eq. (1):

$$WL = \frac{m_i - m_f}{m_i} \quad (1)$$

where *WL* is the weight loss percentage (wt%), m_i is the initial anhydrous weight of wood (g), and m_f is the wood's dry weight post-torrefaction (g).

The weight loss increase was calculated by evaluating the difference between the weight loss for the 0.012 M and the washed one according to an equation used in a previous study (Richa et al., 2023b). The experiments were triplicated, and Pearson's standard deviation of the weight loss was computed. Then, the torrefied wood and untreated wood were similarly cut according to the procedure for surface and core collection (Fig. S1).

2.2. Surface and core characterization using Fourier-transform infrared (FTIR)

The impact of K impregnation and the torrefaction on the surface and core of the beech was analyzed using Fourier transform infrared spectroscopy (FTIR). The device used is the *Nicolet iS10 spectrometer* equipped with an attenuated total reflectance. All samples were analyzed for the surface and core, including all the torrefaction durations (i.e., 5, 15, 30, and 60 min) and all the K concentrations (washed, raw, and impregnated). The FTIR spectra were the average of 64 scans and normalized according to the C–H stretch at 2900 cm^{-1} (Gonultas and Candan, 2018). The measurements were performed on all samples post-torrefaction. The surface and core were extracted after the thermal treatment and then ground to fine particles for the FTIR analysis.

2.3. Pyrolysis and combustion

The behavior of untreated and torrefied wood during pyrolysis and combustion was analyzed using thermogravimetric analysis (TGA2, Mettler-Toledo). It is a highly precise thermal balance, where the atmosphere (N_2 or air) and the temperature can be controlled, and the weight of the sample is recorded throughout the experiment. The same heating profile was used for pyrolysis and combustion, using 100 mL·min^{-1} of N_2 in the case of pyrolysis and 100 mL·min^{-1} of air for the combustion. Oven-dried powder (5 ± 1 mg) was loaded in an alumina crucible and heated from room temperature to 105 °C, where residual moisture was removed for 15 min. The sample was then heated at a heating rate of 20 °C·min^{-1} (Lu and Chen, 2015) until 850 °C. The curve of solid weight percentage as a function of temperature was obtained (TG), and the derivative of the TG (DTG) as a function of time was calculated. The pyrolysis experiments were duplicated, the combustion ones were triplicated, and the average curves were presented. The pyrolysis aims to assess changes during torrefaction along the sample's thickness, torrefaction duration, and potassium content. At the same time, the combustion is to test the effects in an oxidative atmosphere and comprehend the consequences on the stability and reactivity of the wood. The combustion behavior is characterized by the ignition and char burnout temperature. A higher ignition temperature means safer storage and delivery of biofuel. The burnout is linked to the reactivity of the wood, where a higher burnout temperature means it is more stable. The temperature corresponds to almost complete fuel consumption (Lu and Chen, 2015). These parameters were calculated using the intersection method often adopted in the literature (Safar et al., 2019). The mean value for each parameter was presented along with the standard deviation.

2.4. Regression analysis

Regression analysis is a statistical method used for determining the correlations between variables. A regression analysis was performed to better understand the impact of potassium content, torrefaction duration, and the position of the particles (surface or core) on the maximum devolatilization temperature. Determining this temperature is useful in torrefaction to ensure that the hemicelluloses and celluloses are degraded, leading to lower volatile content and higher heating value of the wood (Chen et al., 2021b). The duration and K content of the samples were normalized between 0 and 1 according to the following Eq. (2):

$$X' = \frac{X_i - X_{min}}{X_{max} - X_{min}} \quad (2)$$

where X' is the normalized variable (duration or K content) between 0 and 1; X_i, X_{min}, and X_{max} are the value of *i*, the minimum value, and the maximum value (either in min for the duration or in wt% for K content), respectively.

The peak temperature, the temperature corresponding to the DTG_{max} for pyrolysis, was labeled by T_p. Linear and quadratic regressions were tested to determine the best method for predicting the T_p. The regression was done on the surface data, the core data, and then on the complete data set of the surface and core by making a regression model that predicts the T_p based on the experimental T_p achieved for each K content and duration.

3. Results and discussion

3.1. Impregnation and torrefaction

The impregnation results are presented in Table 1. Even for the impregnated wood, the K content range corresponds to what is naturally present in beech (Glavac et al., 1990). The washing conditions applied were insufficient to demineralize the biomass from the water-soluble K throughout the wood board. A higher K content was obtained at the surface of the washed and raw wood. The core samples all had less K than the surface, regardless of the K content in the impregnation solution. This implies that the heat treatment would be heterogeneous, and the wood probably cannot be considered homogeneous for modeling purposes. Further, the surface is expected to degrade faster than the core during torrefaction, given the catalytic action of potassium (Safar et al., 2019). After heat treatment, with the increased wood weight loss, the potassium content relatively increased to 0.338 % and 0.224 %, respectively, for the surface and core of the 0.012 M sample after 60 min torrefaction. This is in accordance with the corresponding weight loss (32.78 wt%, Table 2), meaning that the K content did not decrease after torrefaction. In other words, the K content obtained after impregnation remained in the wood throughout the torrefaction. This agrees with the literature stating that potassium does not volatilize at low temperatures, including the one used in this study (Zhang et al., 2020c). Since K remains in the torrefied wood, it can be valorized for soil amendment and as a valuable nutrient for plant growth.

The weight results for the bulk samples are presented in Table 2 and Fig. S2a, while Fig. S2b shows the real samples before and after torrefaction. The results proved that the effect of potassium on wood torrefaction was visible for wood boards. Despite the heterogeneity in K content between the surface and the core, the weight loss of the whole sample was accentuated by increased K content. For instance, the weight loss was increased by 23 % between the washed and 0.012 M samples after 30 min torrefaction. This demonstrates the catalytic effect of potassium in the wood boards reported in the wood powder literature (Safar et al., 2019; Silveira et al., 2021b). This is attributed to the role of potassium in facilitating the thermal degradation of cellulose and hemicelluloses and shifting their degradation range to a lower temperature (Richa et al., 2023a). The other torrefaction durations showed the same tendency, with an improved weight loss between the washed and the 0.012 M samples. The weight loss improvement was also shown in Table 2 with a comparison to a study (Richa et al., 2023b) done using the same material and procedure but at 300 °C instead of 275 °C. The results showed that potassium's catalytic action was more efficient at higher temperatures, as observed by the higher weight loss increase at 300 °C. However, after 60 min torrefaction, the efficiency of K becomes lower at 300 °C compared to 275 °C. This is because, at this point (~60% WL at 300 °C), most of the celluloses and hemicelluloses have been degraded by K, meaning that it could no longer catalyze the thermal degradation of the wood, thus reaching the extent of the catalytic torrefaction.

Table 1
Potassium contents for raw and impregnated beech wood.

Sample	Position	K (wt% db)
Washed	Surface	0.094
	Core	0.059
Raw	Surface	0.088
	Core	0.064
0.004 M	Surface	0.141
	Core	0.077
0.008 M	Surface	0.159
	Core	0.082
0.012 M	Surface	0.195
	Core	0.091

Table 2
Bulk beech blocks' weight loss according to potassium content and torrefaction duration.

Sample	WL (wt%)			
	5 min	15 min	30 min	60 min
Washed	14.70 (1.25)[a]	21.95 (0.36)	24.56 (1.38)	28.61 (0.56)
Raw	15.00 (0.88)	22.80 (0.90)	25.68 (0.54)	28.47 (0.81)
0.004 M	15.55 (0.73)	23.11 (0.14)	27.48 (1.26)	30.29 (0.70)
0.008 M	17.14 (0.45)	23.89 (0.37)	29.49 (0.78)	31.57 (0.24)
0.012 M	17.63 (0.84)	24.73 (0.26)	30.11 (0.16)	32.78 (0.83)
$WL_{increase}$ (%) 275 °C	19.93	12.67	22.60	14.58
$WL_{increase}$ (%) 300 °C[b]	20.54	18.69	27.17	11.46

[a] Pearson standard deviation.
[b] obtained from the literature (Richa et al., 2023b).

3.2. Fourier-transform infrared (FTIR)

The FTIR spectra after torrefaction are presented in Fig. 1. No significant differences were observed for the lower torrefaction durations (Fig. 1a and b), regardless of the location in the board (surface or core). However, for the severe torrefaction (60 min), the increased potassium content mainly impacted the –OH stretch (3350 cm^{-1}) and C–O deformation (1027 cm^{-1}) (Gonultas and Candan, 2018). The impact of torrefaction on –OH and C–O stretches was reported in the literature temperatures starting at 280 °C (Ong et al., 2021). The –OH stretch was attributed to alcohol and phenols (Ong et al., 2020). The C–O signal decrease could be attributed to several phenomena, such as depolymerization by homolytic splitting of glycosidic bonds and hydrolysis and strong polycondensation of hemicelluloses (Zheng et al., 2015). A smaller effect was observed in 1400-1150 cm^{-1}, most visible for the core samples after 60 min of torrefaction (Fig. 1d). This band was attributed to C–O–C glycosidic linkages from celluloses and the decomposition of xylan (Wannapeera et al., 2011). In addition to torrefaction, K^+ breaks the glycosidic linkages, inhibiting levoglucosan production and decreasing tar formation (Macedo et al., 2018). Therefore, the higher the K content, the more the wood is degraded (decrease of –OH, C–O, and C–O–C bands).

Small variations in the 1600-1580 cm-1 range also correspond to C=C and C=O stretches (Li et al., 2022). It is perceived that this peak increased slightly in the core with K after 5 min torrefaction, suggesting an improved carbohydrate degradation and the presence of condensed guaiacyl units (Park et al., 2013). However, when increasing the torrefaction duration to 60 min and with the presence of K, this peak decreased. This could be due to the reduced mobility of aromatic carbon while increasing the graphitization degree of the produced biochar (Chen et al., 2023). Other peaks between 1800 and 1550 cm^{-1} are related to acids and amines that undergo O=H stretching and N–H bending (Stevanic and Salmén, 2008). However, no visible changes between the different experiments were observed at this range. Fig. 1e shows the differences between the FTIR spectra of the surface and core of the raw wood torrefied at 275 °C for 60 min. Due to the results' similarity to the raw, the corresponding spectra for the other concentrations were not presented in the figure (Fig. S3). Regardless of the

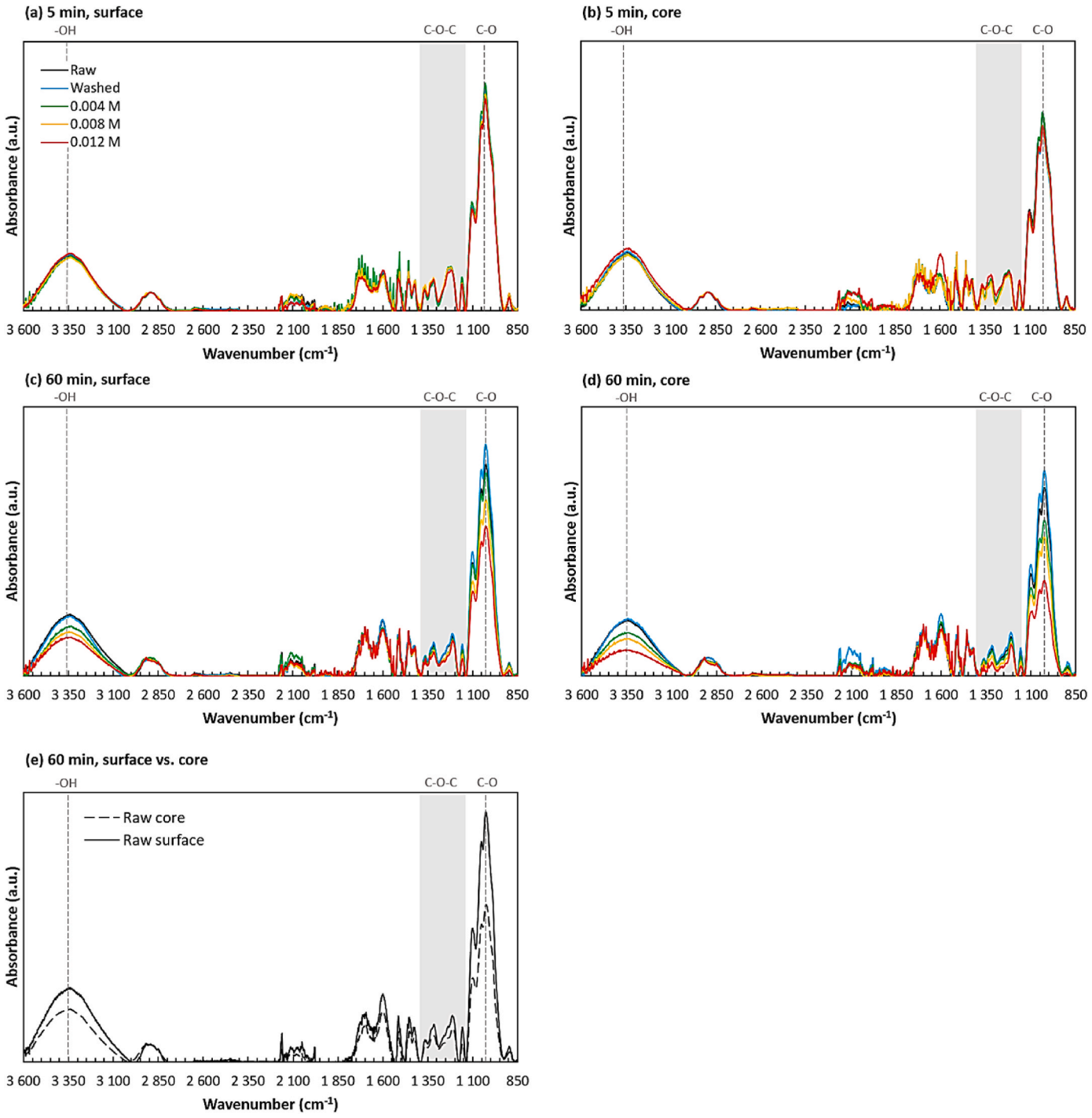

Fig. 1. FTIR spectra of raw and potassium-impregnated samples after torrefaction at 275 °C for 5 min (a and b) and 60 min (c and d), (e) comparison between surface and core.

potassium content in the wood, the core had fewer glycosidic and –OH bonds, except for the washed sample, which showed no difference. The raw sample also exhibited this behavior despite the small differences in potassium content between the surface and core. This leads to the speculation that even the smallest amount of potassium in the sample influenced the wood's decomposition (Safar et al., 2019). This impact could be magnified in the core due to the increased exothermicity with potassium, which primarily degrades hemicelluloses and cellulose (Macedo et al., 2018). It could show that the exothermicity and potassium content increases have a combined effect on wood degradation. Consequently, despite the lower K content at the core, the heart seemed to be more intensely degraded than the surface for all concentrations. This phenomenon is portrayed by the decrease in –OH and C–O peak intensities. The peak located at approximately 3350 cm^{-1} corresponds to the intramolecular hydrogen bonds identified as crystalline cellulose's peak in native wood (Martín-Lara et al., 2017). Therefore, a lower peak intensity indicates degradation of crystalline cellulose for the core samples compared to the surface (Fig. 1e and Fig. S3), and for the K-enriched samples compared to the washed (Fig. 1a–d).

3.3. Pyrolysis

The pyrolysis using TGA helps to characterize the thermal degradation of the untreated and torrefied wood. It is also used to qualitatively analyze the extent of the lignocellulosic materials' decomposition impacted by the torrefaction and potassium content. Until 30 min torrefaction, no notable differences were observed between the different potassium concentrations or between the surface and core (Figs. S4–6). However, similar differences were observed for 30 and 60 min and were more accentuated at 60 min (Figs. S7–8). The TG and DTG curves of the 60 min torrefaction are shown in Figs. 2–3. The solid yield increased with the increasing torrefaction extent (as a function of duration and K-content). The higher char yield is a result of the increased cross-linking reactions during torrefaction, which also decreases the tar yield due to fewer volatiles remaining (Dai et al., 2019). Additionally, the increase in potassium content promotes char formation during pyrolysis (Eom et al., 2012).

Most hemicelluloses degraded within only 5 min of torrefaction at 275 °C, as seen by the disappearance of the hemicelluloses' shoulder (Fig. S5). This also applies to smaller-scale studies of Wen et al. (2014) and Chen and Kuo (2011), which noticed a major degradation of hemicelluloses at this temperature range for wood particles. The cellulose peak intensity decreased with increased torrefaction duration from 5 min to 60 min and increased K content from washed to 0.012 M sample (Fig. 2). The core of the potassium-impregnated samples had lower cellulose content, confirming the FTIR findings. Moreover, the 0.012 M sample's core had a relatively higher lignin content (Fig. 3).

Ohliger et al. (2013) stated that the heat of the reaction during torrefaction becomes more exothermic with the increasing temperature and duration of the treatment. Therefore, it can be deduced that the catalytic action of potassium increased the severity of torrefaction (Silveira et al., 2021b), leading to a magnified impact on the exothermicity of the process. Despite the surface having more potassium than the core, the latter was more degraded during the torrefaction. This could be attributed to three phenomena: (1) the produced volatiles during torrefaction remain trapped for a longer period in the wood, which results in more efficient gas-solid contact (Kung and Kalelkar, 1973), (2) the exothermic reactions in the core lead to internal heat generation that is not immediately evacuated (unlike the surface) (Koumoutsakos et al., 2001), and (3) potassium's catalytic action could be more efficient at the higher temperature achieved in the core. This increased exothermicity caused by potassium could be used as an advantage by optimizing the wood board stacking, leading to a self-heating process (Di Blasi et al., 2018; Perré et al., 2013). This would require lower torrefaction temperatures and/or shorter durations, thus reducing the CO_2 production linked to this process.

3.4. Regression analysis

The experimental determination of the impact of torrefaction duration and K content on T_p is shown in Fig. 4. After 5 min torrefaction, T_p at the surface increased compared to the untreated. This could be explained by the fact that at low torrefaction temperatures (duration in this case), the amorphous cellulose starts to degrade and turns into crystalline cellulose, which degrades at higher temperatures (Tian et al., 2020). As the treatment duration and K content increased, T_p decreased due to the deterioration of both amorphous and crystalline cellulose structures (Safar et al., 2019). Although the cellulose in the core was

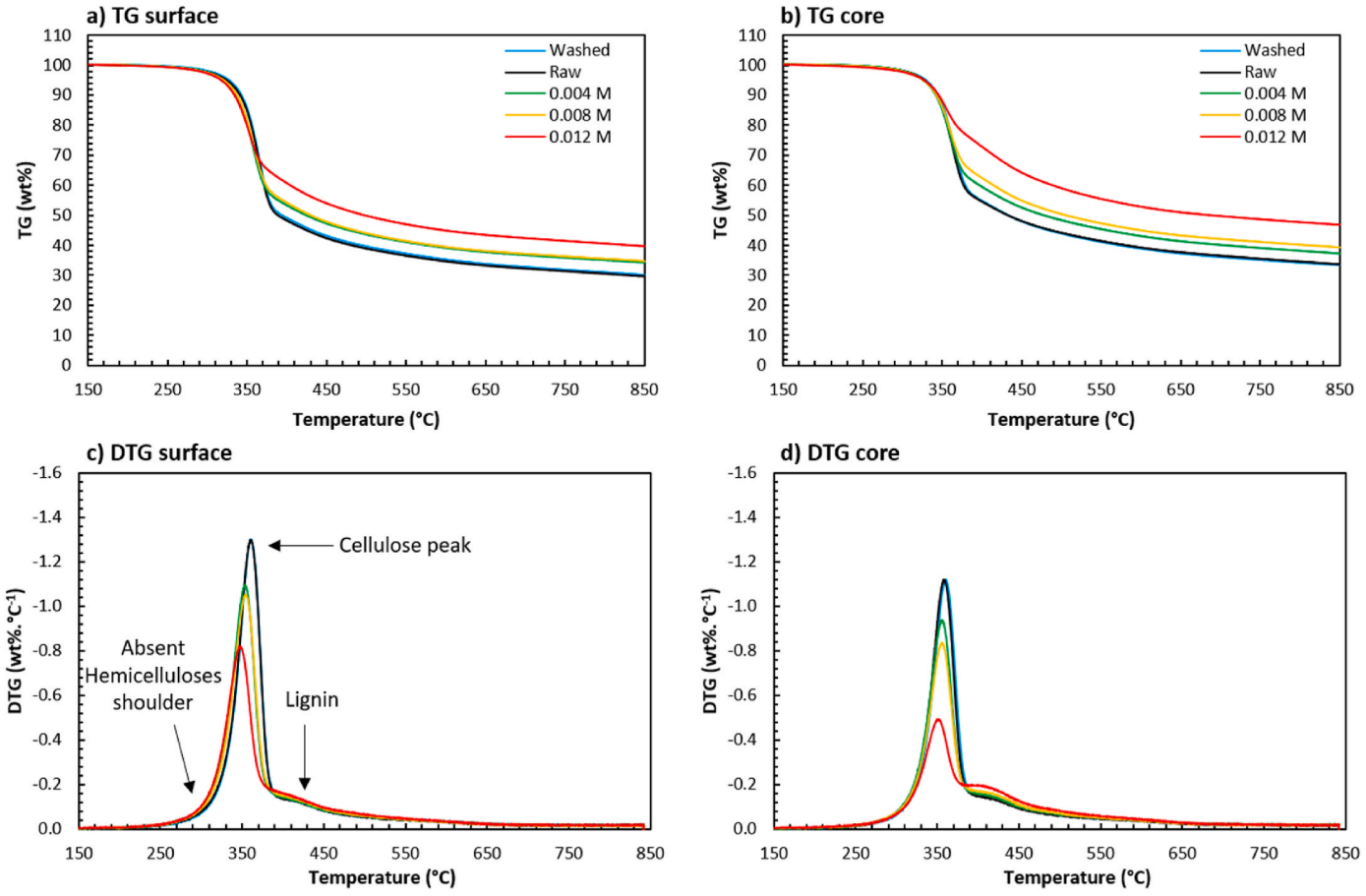

Fig. 2. TG and DTG of the pyrolysis of the surface (a and c) and the core (b and d) extracted from the washed, raw, and K-impregnated wood boards (0.004 M, 0.008 M, and 0.012 M) that underwent a torrefaction for 60 min at 275 °C.

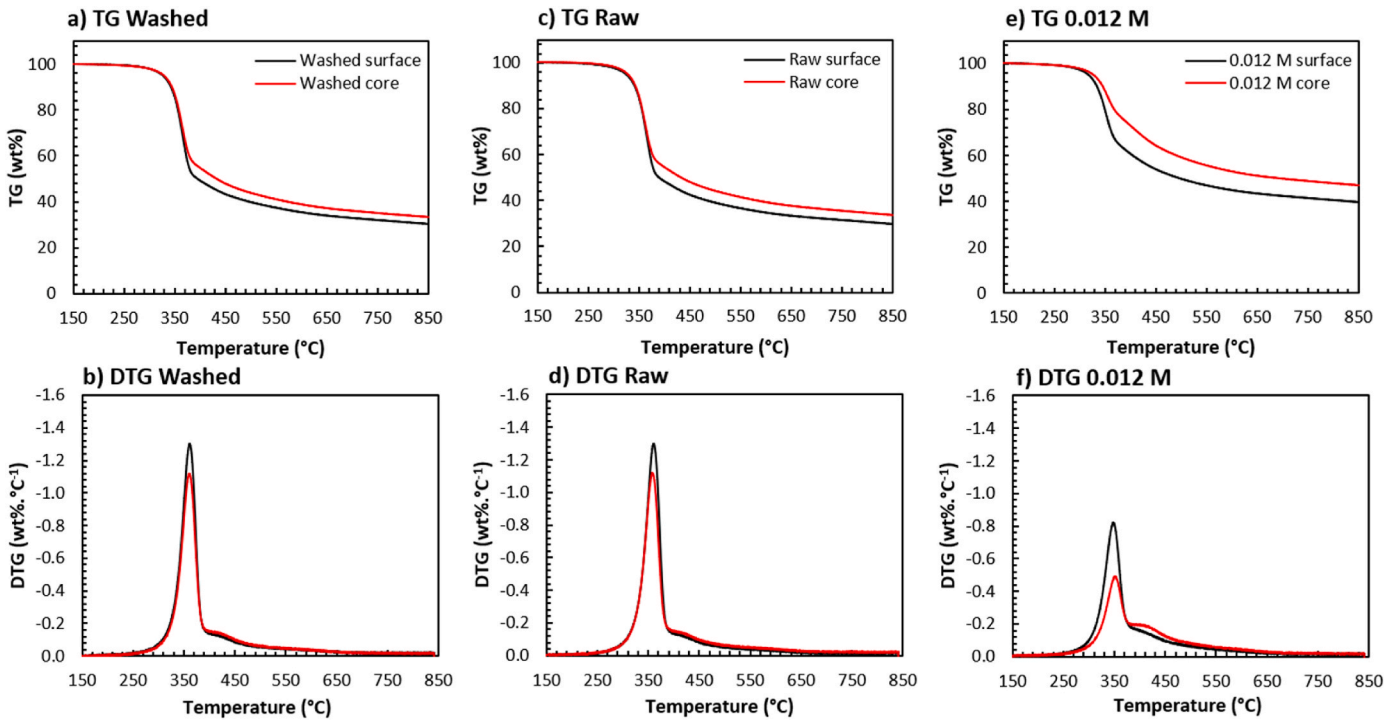

Fig. 3. Comparison between the surface and core of the washed (a–b), raw (c–d), and 0.012 M samples (e–f) during pyrolysis. The surface and core samples were extracted from the wood boards that were torrefied for 60 min at 275 °C.

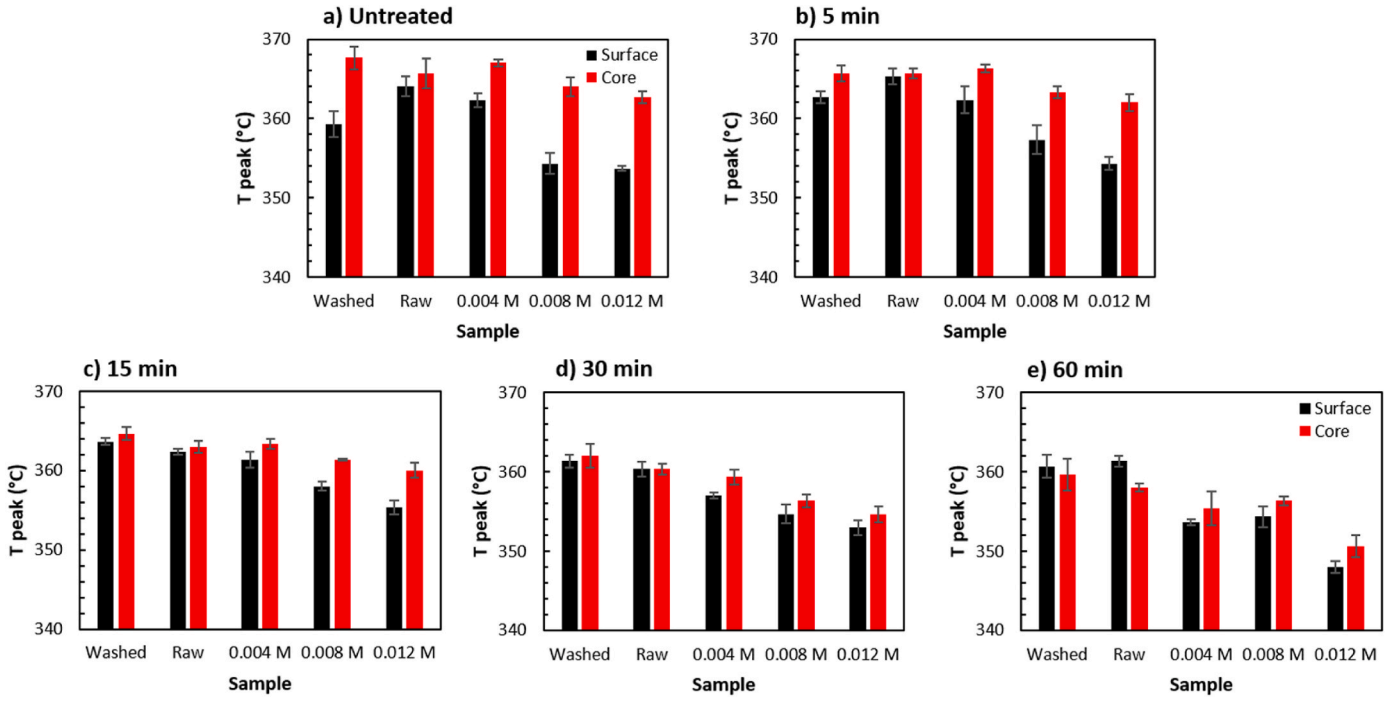

Fig. 4. T_p obtained from the DTG of the pyrolysis experiments at the surface and core of the wood with different K concentrations (washed, raw, 0.004 M, 0.008 M, and 0.012 M) that were previously torrefied for different durations.

more degraded than the surface, T_p was constantly lower at the surface. This evidences the strong impact of potassium on the reduction of T_p by facilitating the degradation of cellulose by shifting its maximum degradation temperature to a lower range.

The estimation of the main degradation temperature based on the K content and torrefaction duration through regression analysis was presented in Table 3. The relative error between the experimental T_p and the predicted one was below 3% for all experiments. This temperature is critical as it corresponds to the highest rate of wood degradation represented by the devolatilization step of hemicelluloses and celluloses. Based on negative coefficients of k' and t' in the linear regression, the potassium content and torrefaction duration tend to decrease the T_p, which correlates with the experimental results obtained. The results showed that a second-order regression was more accurate for predicting

Table 3
Multi-variable first- and second-order regression analysis for T_p prediction.

	1st-order Equation	R^2	σ^a
Surface	$T_p(°C) = 364.23648055 - 4.35004120 \times t' - 9.50981647 \times k'$	0.81889004	1.95791908
Core	$T_p(°C) = 367.51736202 - 9.73344721 \times t' - 5.27128644 \times k'$	0.89114876	1.49205684
Surface + core	$T_p(°C) = 365.73963501 - 7.04174421 \times t' - 9.67379676 \times k'$	0.75983354	2.28985997
	2nd-order Equation	R^2	σ
Surface	$T_p(°C) = 363.09522694 - 0.00262986 \times t' - 5.10104787 \times k' - 3.61915385 \times t'k' - 2.70084095 \times t'^2 - 3.27190666 \times k'^2$	0.84228868	1.96602727
Core	$T_p(°C) = 367.08122878 - 15.14243726 \times t' + 1.04353702 \times k' - 4.26190236 \times t'k' + 7.35361027 \times t'^2 - 4.92040732 \times k'^2$	0.95282343	1.05697906
Surface + core	$T_p(°C) = 365.53488069 - 9.12119090 \times t' - 6.85463020 \times k' + 1.29270645 \times t'k' + 1.42702424 \times t'^2 - 3.593338114 \times k'^2$	0.76336335	2.34918025

[a] σ is the standard deviation calculated by the model.

the change of T_p as a function of the torrefaction duration and K content for both the surface and the core. The regression coefficient R^2 was 0.89 for the surface and 0.95 for the core. However, when combining the data for both surface and core, the model seemed less efficient, with R^2 = 0.76 for both linear and quadratic regression. This proves that T_p depends not only on the torrefaction duration and K content but also on the location along the board's thickness during torrefaction.

Furthermore, both regression methods predicted a higher accuracy of the T_p in the core rather than the surface. At the surface, both 1st- and 2nd-order equations showed a higher impact of K content than torrefaction duration, deduced by comparing nondimensional k' and t' coefficients. Inversely, at the core, the duration had a stronger impact. This correlates with the TG results (section 3.3), where the core was more degraded despite the lower K content. In the core, with the increase of torrefaction duration, the volatile production increases, further degrading the core (Broström et al., 2012). This phenomenon eventually overpowers the potassium's catalytic action. The interaction between K and the duration was correlated through the *k't'* coefficient. There were significant interactions between these two variables with a relatively significant *k't'* coefficient compared to the other coefficients (*k'*, *t'*, k'^2, and t'^2).

3.5. Combustion

The impact of torrefaction and potassium content in an oxidative atmosphere is presented in Fig. 5. The TG and DTG for all the concentrations were also provided in Fig. S9. The combustion occurs in two steps, as identified by the DTG peaks. The first one is the devolatilization step, which corresponds to the degradation of the residual hemicelluloses and cellulose (Aghamohammadi et al., 2011). The temperature range was approximately between 235 °C and 365 °C, depending on the experiment. The second is the char oxidation step and the decomposition of the remaining lignin (Skreiberg et al., 2011). This step occurred at a temperature range of 365 °C–515 °C, depending on the experiment. By comparing the second DTG peaks between the surface (rich in K) and the core, the potassium seemed to catalyze the char oxidation, shifting the peak to lower temperatures. This behavior was reported in the study of Ding et al. (2017) on potassium-impregnated biomass.

According to the oxygen-transfer theory, the potassium partially migrates on the carbon surface and increases the active sites for catalytic reactions (Yu et al., 2021). This weakens the C=C surface bonds and promotes the CO_2 and CO products' desorption (Deng et al., 2018). This phenomenon was less apparent for the raw wood (Fig. 5c–d) since it had the lowest difference in K content between the surface (0.088 %) and core (0.064 %). The surface was less degraded for the K-impregnated samples despite the bigger K content, similar to what was observed in

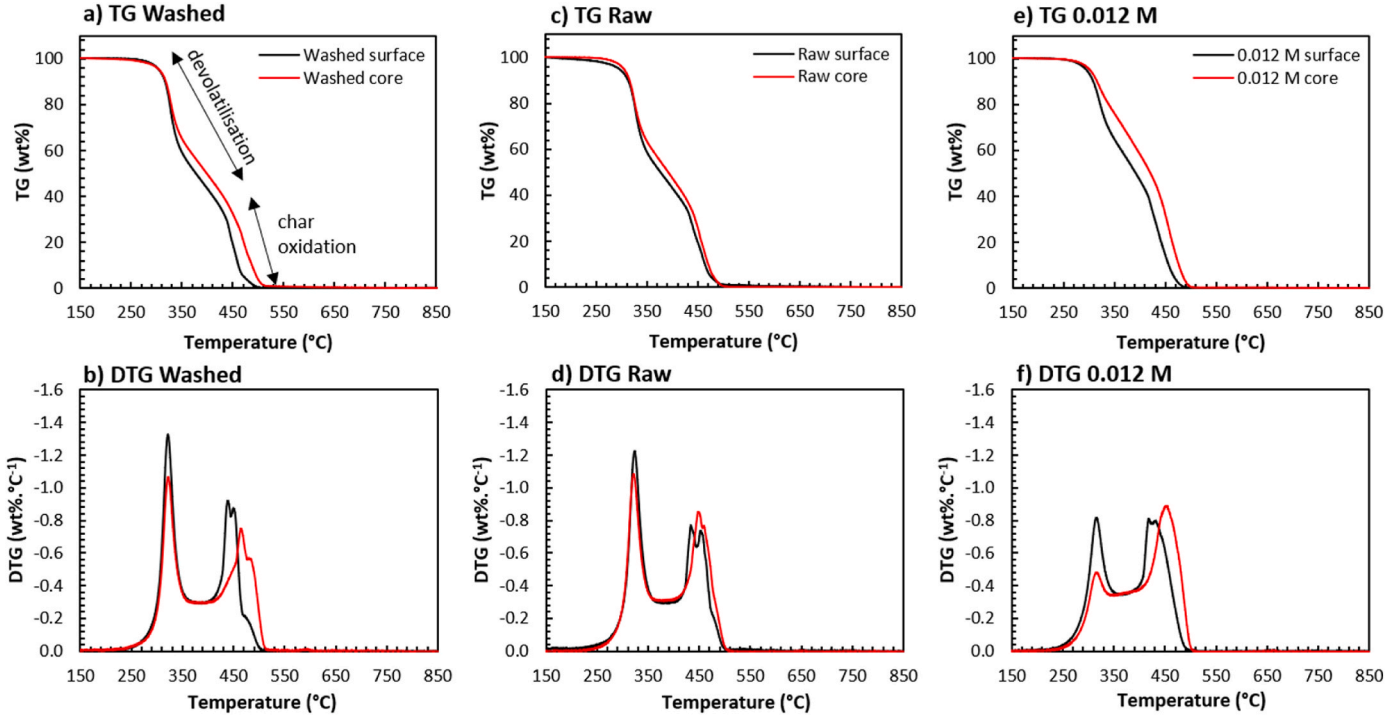

Fig. 5. Comparison between the surface and core of the washed (a–b), raw (c–d), and 0.012 M sample (e–f) during combustion. The surface and core samples were extracted from the wood boards that were torrefied for 60 min at 275 °C.

pyrolysis (Section 3.3). In the core, the volatiles peak was significantly reduced (DTG) to the point where the behavior of the 0.012 M sample became closer to that of coal, which has a more prominent char combustion peak. This is due to the stronger degradation of the core during the torrefaction that leaves a lower volatile matter content, thus reducing the first peak intensity. As the intensity of the first peak (devolatilization) becomes close to that of the second peak (char oxidation), the TG and DTG profiles become close to those of bituminous and anthracite coals. Additionally, the core's char oxidation peaks shifted to higher temperatures, indicating a higher quality of combustion. Biomass must have properties close to coal to achieve synergy upon co-firing (Valix et al., 2017). Plus, as the obtained wood can either replace coal or be used in co-firing, it significantly reduces the environmental pollution from coal combustion. For the washed and raw wood, the first peak's intensity was higher than the second one. However, with the increase of K content to 0.012 M sample, the second peak became the most intense one. This is attributed to the combined action of potassium's catalytic effect and the exothermic reactions in the core that promote the devolatilization during the previous torrefaction step. It should be noted that a minor devolatilization peak means that the wood has lower volatile matter content, which is correlated to lower particulate matter emissions (Itoh et al., 2020). Consequently, catalytic torrefaction as a pretreatment reduces pollution from the combustion process.

The combustion parameters were obtained from the TG and DTG curves for untreated and torrefied wood (Figs. S10–11) and are displayed in Fig. 6. The main volatiles' degradation temperature corresponds to the first local DTG_{max} peak (T_{p1}). T_{p1} decreased with torrefaction and the K-impregnation. The increase of K content decreased the combustion peak temperature (T_{p2}). The untreated surface was reduced by 9% between the washed and the 0.012 M compared to 3% for the core. The torrefied wood's T_{p2} was reduced by 4.5% and 2.5% for the surface and core, respectively. This correlated with the catalytic effect of potassium on the char combustion stage reported in the literature (Jones et al., 2007). Before torrefaction, the potassium content in the sample greatly impacted the ignition temperature (*Ti*) (Fig. 6e). The effect is marked by the difference between the surface and core, where the 0.012 M sample had a T_i of 276 °C at the surface (0.195 wt%K) and 292 °C at the core (0.091 wt%K). Torrefaction increased T_i and reduced the gradient between the surface and core. This could be because after 60 min torrefaction, the light volatiles have been released, forming a more stable structure requiring more energy for the reaction (Ma et al., 2022). This decreases the wood's self-ignition risk, leading to safe storage conditions. Similarly to T_i, the char burnout temperature (T_b) was higher for the core samples (lower K content) and was improved by torrefaction, which brings it closer to coal's range (359–611 °C) (Valix et al., 2017). In this study, T_b shifted from 454-477 °C to 470–500 °C after 60 min torrefaction. Therefore, it can be deduced that potassium addition increased the reactivity of the wood while torrefaction and water washing decreased it.

3.6. Limitations and perspectives

The study highlighted the benefits of large-scale catalytic torrefaction and led to a deeper understanding of potassium's role during the torrefaction of wood boards. However, the work also showed weaknesses in this process that must be addressed. Since the impregnation and the torrefaction were not homogeneous, the application field of the produced biochar should be carefully considered. If it is desired to obtain a biochar with uniform properties, then this process requires some improvements, such as using thinner boards. The presence of potassium seems to lead to self-heating properties, especially in the core, where heat is not easily dissipated. This could be turned into an advantage by stacking the K-impregnated boards for torrefaction, thus delaying the heat dissipation between the boards and promoting the self-heating effect. By doing so in a controlled way, lower temperatures or

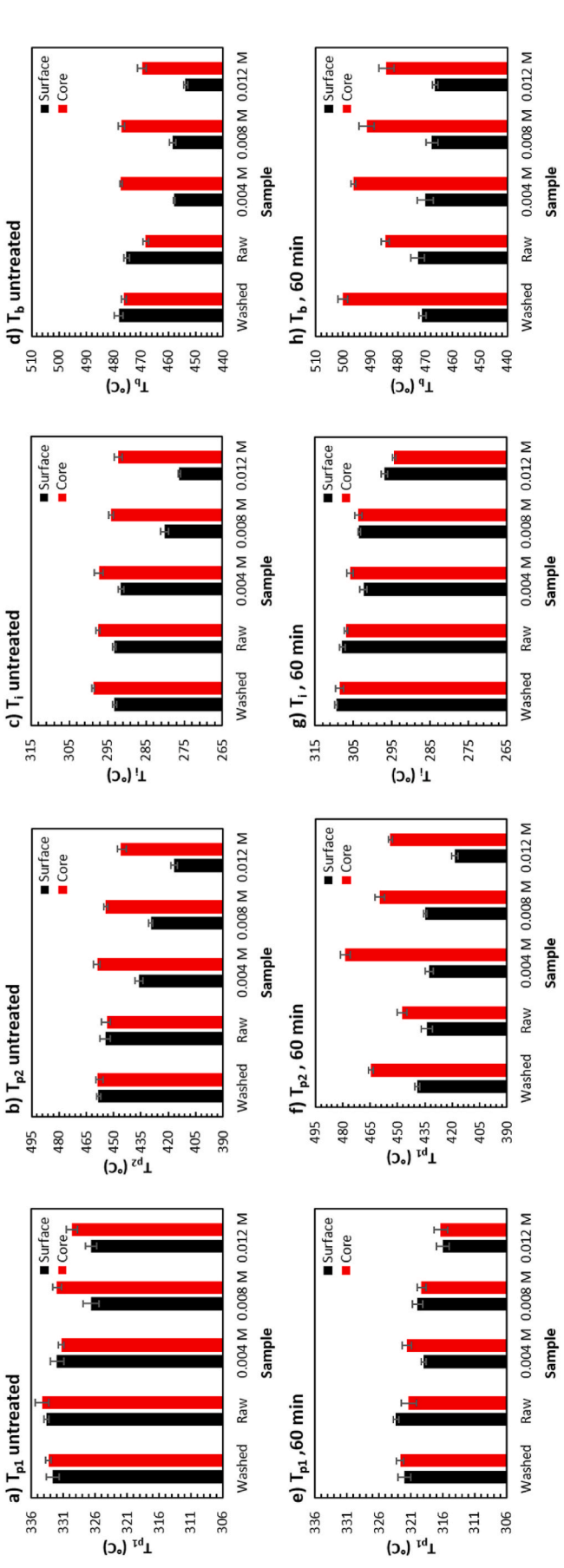

Fig. 6. Combustion parameters determined from the thermogravimetric analysis of untreated (a–d) and torrefied wood (e–h) for the samples with different K content (washed, raw, 0.004 M, 0.008 M, and 0.012 M).

duration of the treatments can be used, thereby reducing emissions. Therefore, it is advised to adjust the furnaces for this large-scale application and model the heat transfer between the boards to optimize the process. Additionally, for future work, the produced biochar from pyrolysis and combustion should be characterized (porosity, structure, surface area, etc.). Then, its efficiency in removing pollutants from water and the air and its capacity for soil remediation should be evaluated.

4. Conclusions

Torrefaction of K-impregnated wood is a promising solution to decrease environmental pollution linked to energy production (from coal or raw biomass). Therefore, a novel study evaluated the changes that occur during the catalytic torrefaction of waste wood boards. ICP-AES results showed that the surface retained more K than the core after impregnation. Torrefaction coupled with K strongly affected the glycosidic bonds and the –OH stretch. The glygosidic bond cleavage is attributed to the catalytic action of potassium in facilitating the thermal degradation of cellulose. Potassium also seems to increase the graphitization degree of the produced biochar slightly. The torrefied wood's core was more degraded than the surface despite the lower K content due to the lingering of the exothermic reactions. The catalytic action of potassium was stronger in the core due to a lower rate of volatile mass transfer. Therefore, by impacting the mass and heat transfer, the thickness of the wood board plays an important role in the thermal degradation behavior of the wood boards. Catalytic torrefaction produces wood with lower volatile matter and better char oxidation during combustion. During pyrolysis, torrefaction reduced the differences in T_p between the surface and core, leading to more homogeneous properties in the wood board. A regression analysis on the T_p showed a visible interaction between potassium and the torrefaction duration. Moreover, torrefaction and water-washing increased wood's stability in combustion.

Credit author statement

Larissa Richa: Formal analysis, Methodology, Validation, Writing – original draft. Baptiste Colin: Conceptualization, Project administration and Supervision, and writing-review editing of the manuscript. Anelie Pétrissans: Conceptualization, Funding acquisition, Project administration and Supervision, and writing-review editing of the manuscript. Jasmine Wolfgram: Data acquisition, Methodology. Ciera Wallace: Data acquisition, Methodology. Rafael L. Quirino: Validation, writing-review editing of the manuscript. Wei-Hsin Chen: Conceptualization, Validation, Project administration, writing-review editing of the manuscript. Mathieu Pétrissans: Funding acquisition, Project administration and Supervision, and writing-review editing of the manuscript.

Declaration of competing interest

The authors declare that they have no known competing financial interests or personal relationships that could have appeared to influence the work reported in this paper.

Data availability

Data will be made available on request.

Acknowledgments

The authors gratefully acknowledge the financial support under the program ANR-11-LABEX-0002-01 (Lab of Excellence ARBRE) in France, the National Science Foundation (NSF) under the grant NSF-IRES 1952402 (I-CEMITURE (International-CEMITURE)) awarded by the NSF Office of International Science & Engineering (OISE), Georgia Southern University USA; Thomas Jefferson Fund of the Embassy of France in the United States and the FACE Foundation. The authors also acknowledge the financial support of the National Science and Technology Council, Taiwan, R.O.C., under contracts NSTC 112-2218-E-006-025- and NSTC 112-2218-E-002-052- for this research.

Appendix A. Supplementary data

Supplementary data to this article can be found online at https://doi.org/10.1016/j.envpol.2023.122911.

References

Aghamohammadi, N., Nik Sulaiman, N.M., Aroua, M.K., 2011. Combustion characteristics of biomass in SouthEast Asia. Biomass Bioenergy 35, 3884–3890. https://doi.org/10.1016/j.biombioe.2011.06.022.

Aniza, R., Chen, W.-H., Pétrissans, A., Hoang, A.T., Ashokkumar, V., Pétrissans, M., 2023. A review of biowaste remediation and valorization for environmental sustainability: artificial intelligence approach. Environ. Pollut. 324, 121363 https://doi.org/10.1016/j.envpol.2023.121363.

Bates, R.B., Ghoniem, A.F., 2013. Biomass torrefaction: modeling of reaction thermochemistry. Bioresour. Technol. 134, 331–340. https://doi.org/10.1016/j.biortech.2013.01.158.

Broström, M., Nordin, A., Pommer, L., Branca, C., Di Blasi, C., 2012. Influence of torrefaction on the devolatilization and oxidation kinetics of wood. J. Anal. Appl. Pyrolysis 96, 100–109. https://doi.org/10.1016/j.jaap.2012.03.011.

Buhani, Suharso, Rilyanti, M., Antika, F.D.R., Lestari, L.P., Sumadi Ansori, M., Elwakeel, K.Z., 2023. Functionalization of carbon from rubber fruit shells (Hevea brasiliensis) with silane agents and its application to the adsorption of bi-component mixtures of methylene blue and crystal violet. Environ. Sci. Pollut. Res. https://doi.org/10.1007/s11356-023-28031-9.

Chai, M., Xie, L., Yu, X., Zhang, X., Yang, Y., Rahman, MdM., Blanco, P.H., Liu, R., Bridgwater, A.V., Cai, J., 2021. Poplar wood torrefaction: kinetics, thermochemistry and implications. Renew. Sustain. Energy Rev. 143, 110962 https://doi.org/10.1016/j.rser.2021.110962.

Chen, W.-H., Kuo, P.-C., 2011. Isothermal torrefaction kinetics of hemicellulose, cellulose, lignin and xylan using thermogravimetric analysis. Energy 36, 6451–6460. https://doi.org/10.1016/j.energy.2011.09.022.

Chen, W.-H., Lin, B.-J., Lin, Y.-Y., Chu, Y.-S., Ubando, A.T., Show, P.L., Ong, H.C., Chang, J.-S., Ho, S.-H., Culaba, A.B., Pétrissans, A., Pétrissans, M., 2021a. Progress in biomass torrefaction: principles, applications and challenges. Prog. Energy Combust. Sci. 82, 100887 https://doi.org/10.1016/j.pecs.2020.100887.

Chen, C., Chen, W., Ilham, Z., 2021b. Effects of torrefaction and water washing on the properties and combustion reactivity of various wastes. Int. J. Energy Res. 45, 8125–8139. https://doi.org/10.1002/er.5458.

Chen, Z., Lai, C., Qin, L., Li, L., Yang, L., Liu, S., Zhang, M., Zhou, X., Xu, F., Yan, H., Tang, C., Qian, S., Sun, Q., 2023. Synergy between graphitized biochar and goethite driving efficient H2O2 activation: enhanced performance and mechanism analysis. Sep. Purif. Technol. 314, 123516 https://doi.org/10.1016/j.seppur.2023.123516.

Dai, L., Wang, Y., Liu, Y., Ruan, R., He, C., Yu, Z., Jiang, L., Zeng, Z., Tian, X., 2019. Integrated process of lignocellulosic biomass torrefaction and pyrolysis for upgrading bio-oil production: a state-of-the-art review. Renew. Sustain. Energy Rev. 107, 20–36. https://doi.org/10.1016/j.rser.2019.02.015.

Deng, S., Wang, X., Zhang, J., Liu, Z., Mikulčić, H., Vujanović, M., Tan, H., Duić, N., 2018. A kinetic study on the catalysis of KCl, K2SO4, and K2CO3 during oxy-biomass combustion. J. Environ. Manag. 218, 50–58. https://doi.org/10.1016/j.jenvman.2018.04.057.

Di Blasi, C., Branca, C., Galgano, A., 2018. Role of the potassium chemical state in the global exothermicity of wood pyrolysis. Ind. Eng. Chem. Res. 57, 11561–11571. https://doi.org/10.1021/acs.iecr.8b02047.

Ding, M., Wei, B., Zhang, Z., She, S., Huang, L., Ge, S., Sheng, L., 2017. Effect of potassium organic and inorganic salts on thermal decomposition of reconstituted tobacco sheet. J. Therm. Anal. Calorim. 129, 975–984. https://doi.org/10.1007/s10973-017-6214-7.

Elgarahy, A.M., Mostafa, H.Y., Zaki, E.G., ElSaeed, S.M., Elwakeel, K.Z., Akhdhar, A., Guibal, E., 2023. Methylene blue removal from aqueous solutions using a biochar/gellan gum hydrogel composite: effect of agitation mode on sorption kinetics. Int. J. Biol. Macromol. 232, 123355 https://doi.org/10.1016/j.ijbiomac.2023.123355.

Elwakeel, K.Z., El-Sayed, G.O., Abo El-Nassr, S.M., 2015. Removal of ferrous and manganous from water by activated carbon obtained from sugarcane bagasse. Desalination Water Treat. 55, 471–483. https://doi.org/10.1080/19443994.2014.919606.

Eom, I.-Y., Kim, J.-Y., Kim, T.-S., Lee, S.-M., Choi, D., Choi, I.-G., Choi, J.-W., 2012. Effect of essential inorganic metals on primary thermal degradation of lignocellulosic biomass. Bioresour. Technol. 104, 687–694. https://doi.org/10.1016/j.biortech.2011.10.035.

Florez, D., Stéphan, A., Perré, P., Rémond, R., 2023. Probabilistic multi-objective optimization of wood torrefaction conditions using a validated mechanistic model. Fuel 335, 126932. https://doi.org/10.1016/j.fuel.2022.126932.

Glavac, V., Koenies, H., Ebben, U., 1990. Seasonal variation of calcium, magnesium, potassium, and manganese contents in xylem sap of beech(Fagus sylvatica L.) in a 35-year-old limestone beech forest stand. Trees 4. https://doi.org/10.1007/BF00226069.

Gonultas, O., Candan, Z., 2018. Chemical characterization and ftir spectroscopy of thermally compressed eucalyptus wood panels. Maderas Cienc. Tecnol. https://doi.org/10.4067/S0718-221X2018005031301.
Guo, F., Liu, Y., Wang, Y., Li, X., Li, T., Guo, C., 2016. Pyrolysis kinetics and behavior of potassium-impregnated pine wood in TGA and a fixed-bed reactor. Energy Convers. Manag. 130, 184–191. https://doi.org/10.1016/j.enconman.2016.10.055.
Itoh, T., Fujiwara, N., Iwabuchi, K., Narita, T., Mendbayar, D., Kamide, M., Niwa, S., Matsumi, Y., 2020. Effects of pyrolysis temperature and feedstock type on particulate matter emission characteristics during biochar combustion. Fuel Process. Technol. 204, 106408 https://doi.org/10.1016/j.fuproc.2020.106408.
Jones, J.M., Darvell, L.I., Bridgeman, T.G., Pourkashanian, M., Williams, A., 2007. An investigation of the thermal and catalytic behaviour of potassium in biomass combustion. Proc. Combust. Inst. 31, 1955–1963. https://doi.org/10.1016/j.proci.2006.07.093.
Kassman, H., Broström, M., Berg, M., Åmand, L.-E., 2011. Measures to reduce chlorine in deposits: application in a large-scale circulating fluidised bed boiler firing biomass. Fuel 90, 1325–1334. https://doi.org/10.1016/j.fuel.2010.12.005.
Khazraie Shoulaifar, T., DeMartini, N., Karlström, O., Hemming, J., Hupa, M., 2016. Impact of organically bonded potassium on torrefaction: Part 2. Modeling. Fuel 168, 107–115. https://doi.org/10.1016/j.fuel.2015.11.084.
Kota, K.B., Shenbagaraj, S., Sharma, P.K., Sharma, A.K., Ghodke, P.K., Chen, W.-H., 2022. Biomass torrefaction: an overview of process and technology assessment based on global readiness level. Fuel 324, 124663. https://doi.org/10.1016/j.fuel.2022.124663.
Koumoutsakos, A., Avramidis, S., Hatzikiriakos, S.G., 2001. Radio frequency vacuum drying of wood. I. Mathematical model. Dry. Technol. 19, 65–84. https://doi.org/10.1081/DRT-100001352.
Kumar, L., Koukoulas, A.A., Mani, S., Satyavolu, J., 2017. Integrating torrefaction in the wood pellet industry: a critical review. Energy Fuels 31, 37–54. https://doi.org/10.1021/acs.energyfuels.6b02803.
Kung, H.-C., Kalelkar, A.S., 1973. On the heat of reaction in wood pyrolysis. Combust. Flame 20, 91–103. https://doi.org/10.1016/S0010-2180(73)81260-X.
Lee, K.-T., Shih, Y.-T., Rajendran, S., Park, Y.-K., Chen, W.-H., 2023. Spent coffee ground torrefaction for waste remediation and valorization. Environ. Pollut. 324, 121330 https://doi.org/10.1016/j.envpol.2023.121330.
Li, K., Li, J., Qin, F., Dong, H., Wang, W., Luo, H., Qin, D., Zhang, C., Tan, H., 2023a. Nano zero valent iron in the 21st century: a data-driven visualization and analysis of research topics and trends. J. Clean. Prod. 415, 137812 https://doi.org/10.1016/j.jclepro.2023.137812.
Li, K., Tan, H., Li, J., Li, Z., Qin, F., Luo, H., Qin, D., Weng, H., Zhang, C., 2023b. Unveiling the effects of carbon-based nanomaterials on crop growth: from benefits to detriments. J. Agric. Food Chem. 71, 11860–11874. https://doi.org/10.1021/acs.jafc.3c02768.
Li, L., Cheng, M., Qin, L., Almatrafi, E., Yang, X., Yang, L., Tang, C., Liu, S., Yi, H., Zhang, M., Fu, Y., Zhou, X., Xu, F., Zeng, G., Lai, C., 2022. Enhancing hydrogen peroxide activation of Cu Co layered double hydroxide by compositing with biochar: performance and mechanism. Sci. Total Environ. 828, 154188 https://doi.org/10.1016/j.scitotenv.2022.154188.
Li, Y., Fu, T.-M., Yu, J.Z., Feng, X., Zhang, L., Chen, J., Boreddy, S.K.R., Kawamura, K., Fu, P., Yang, X., Zhu, L., Zeng, Z., 2021. Impacts of chemical degradation on the global budget of atmospheric levoglucosan and its use as a biomass burning tracer. Environ. Sci. Technol. 55, 5525–5536. https://doi.org/10.1021/acs.est.0c07313.
Lu, J.-J., Chen, W.-H., 2015. Investigation on the ignition and burnout temperatures of bamboo and sugarcane bagasse by thermogravimetric analysis. Appl. Energy 160, 49–57. https://doi.org/10.1016/j.apenergy.2015.09.026.
Ma, J., Feng, S., Zhang, Z., Wang, Z., Kong, W., Yuan, P., Shen, B., Mu, L., 2022. Effect of torrefaction pretreatment on the combustion characteristics of the biodried products derived from municipal organic wastes. Energy 239, 122358. https://doi.org/10.1016/j.energy.2021.122358.
Macedo, L.A. de, Commandré, J.-M., Rousset, P., Valette, J., Pétrissans, M., 2018. Influence of potassium carbonate addition on the condensable species released during wood torrefaction. Fuel Process. Technol. 169, 248–257. https://doi.org/10.1016/j.fuproc.2017.10.012.
Macedo, L.A., Silveira, E.A., Rousset, P., Valette, J., Commandré, J.-M., 2022. Synergistic effect of biomass potassium content and oxidative atmosphere: impact on torrefaction severity and released condensables. Energy 254, 124472. https://doi.org/10.1016/j.energy.2022.124472.
Martín-Lara, M.A., Ronda, A., Zamora, M.C., Calero, M., 2017. Torrefaction of olive tree pruning: effect of operating conditions on solid product properties. Fuel 202, 109–117. https://doi.org/10.1016/j.fuel.2017.04.007.
Medic, D., Darr, M., Shah, A., Rahn, S., 2012. Effect of torrefaction on water vapor adsorption properties and resistance to microbial degradation of corn stover. Energy Fuels 26, 2386–2393. https://doi.org/10.1021/ef3000449.
Ohliger, A., Förster, M., Kneer, R., 2013. Torrefaction of beechwood: a parametric study including heat of reaction and grindability. Fuel 104, 607–613. https://doi.org/10.1016/j.fuel.2012.06.112.
Ong, H.C., Chen, W.-H., Singh, Y., Gan, Y.Y., Chen, C.-Y., Show, P.L., 2020. A state-of-the-art review on thermochemical conversion of biomass for biofuel production: a TG-FTIR approach. Energy Convers. Manag. 209, 112634 https://doi.org/10.1016/j.enconman.2020.112634.
Ong, H.C., Yu, K.L., Chen, W.-H., Pillejera, M.K., Bi, X., Tran, K.-Q., Pétrissans, A., Pétrissans, M., 2021. Variation of lignocellulosic biomass structure from torrefaction: a critical review. Renew. Sustain. Energy Rev. 152, 111698 https://doi.org/10.1016/j.rser.2021.111698.
Park, J., Meng, J., Lim, K.H., Rojas, O.J., Park, S., 2013. Transformation of lignocellulosic biomass during torrefaction. J. Anal. Appl. Pyrolysis 100, 199–206. https://doi.org/10.1016/j.jaap.2012.12.024.
Perré, P., Rémond, R., Turner, I., 2013. A comprehensive dual-scale wood torrefaction model: application to the analysis of thermal run-away in industrial heat treatment processes. Int. J. Heat Mass Tran. 64, 838–849. https://doi.org/10.1016/j.ijheatmasstransfer.2013.03.066.
Rath, J., 2003. Heat of wood pyrolysis. Fuel 82, 81–91. https://doi.org/10.1016/S0016-2361(02)00138-2.
Richa, L., Colin, B., Pétrissans, A., Wallace, C., Hulette, A., Quirino, R.L., Chen, W.-H., Pétrissans, M., 2023a. Catalytic and char-promoting effects of potassium on lignocellulosic biomass torrefaction and pyrolysis. Environ. Technol. Innov., 103193 https://doi.org/10.1016/j.eti.2023.103193.
Richa, L., Colin, B., Pétrissans, A., Wallace, C., Wolfgram, J., Quirino, R.L., Chen, W.-H., Pétrissans, M., 2023b. Potassium carbonate impregnation and torrefaction of wood block for thermal properties improvement: prediction of torrefaction performance using artificial neural network. Appl. Energy 351, 121894. https://doi.org/10.1016/j.apenergy.2023.121894.
Robey, N.M., Solo-Gabriele, H.M., Jones, A.S., Marini, J., Townsend, T.G., 2018. Metals content of recycled construction and demolition wood before and after implementation of best management practices. Environ. Pollut. 242, 1198–1205. https://doi.org/10.1016/j.envpol.2018.07.134.
Safar, M., Lin, B.-J., Chen, W.-H., Langauer, D., Chang, J.-S., Raclavska, H., Pétrissans, A., Rousset, P., Pétrissans, M., 2019. Catalytic effects of potassium on biomass pyrolysis, combustion and torrefaction. Appl. Energy 235, 346–355. https://doi.org/10.1016/j.apenergy.2018.10.065.
Shen, Y., Zhang, N., Zhang, S., 2020. Catalytic pyrolysis of biomass with potassium compounds for Co-production of high-quality biofuels and porous carbons. Energy 190, 116431. https://doi.org/10.1016/j.energy.2019.116431.
Sher, F., Yaqoob, A., Saeed, F., Zhang, S., Jahan, Z., Klemeš, J.J., 2020. Torrefied biomass fuels as a renewable alternative to coal in co-firing for power generation. Energy 209, 118444. https://doi.org/10.1016/j.energy.2020.118444.
Silveira, E.A., Luz, S., Candelier, K., Macedo, L.A., Rousset, P., 2021a. An assessment of biomass torrefaction severity indexes. Fuel 288, 119631. https://doi.org/10.1016/j.fuel.2020.119631.
Silveira, E.A., Macedo, L.A., Candelier, K., Rousset, P., Commandré, J.-M., 2021b. Assessment of catalytic torrefaction promoted by biomass potassium impregnation through performance indexes. Fuel 304, 121353. https://doi.org/10.1016/j.fuel.2021.121353.
Singh, R.K., Sarkar, A., Chakraborty, J.P., 2020. Effect of torrefaction on the physicochemical properties of eucalyptus derived biofuels: estimation of kinetic parameters and optimizing torrefaction using response surface methodology (RSM). Energy 198, 117369. https://doi.org/10.1016/j.energy.2020.117369.
Skreiberg, A., Skreiberg, Ø., Sandquist, J., Sørum, L., 2011. TGA and macro-TGA characterisation of biomass fuels and fuel mixtures. Fuel 90, 2182–2197. https://doi.org/10.1016/j.fuel.2011.02.012.
Stevanic, J.S., Salmén, L., 2008. Characterizing wood polymers in the primary cell wall of Norway spruce (Picea abies (L.) Karst.) using dynamic FT-IR spectroscopy. Cellulose 15, 285–295. https://doi.org/10.1007/s10570-007-9169-1.
Tian, X., Dai, L., Wang, Y., Zeng, Z., Zhang, S., Jiang, L., Yang, X., Yue, L., Liu, Y., Ruan, R., 2020. Influence of torrefaction pretreatment on corncobs: a study on fundamental characteristics, thermal behavior, and kinetic. Bioresour. Technol. 297, 122490 https://doi.org/10.1016/j.biortech.2019.122490.
Valix, M., Katyal, S., Cheung, W.H., 2017. Combustion of thermochemically torrefied sugar cane bagasse. Bioresour. Technol. 223, 202–209. https://doi.org/10.1016/j.biortech.2016.10.053.
Wannapeera, J., Fungtammasan, B., Worasuwannarak, N., 2011. Effects of temperature and holding time during torrefaction on the pyrolysis behaviors of woody biomass. J. Anal. Appl. Pyrolysis 92, 99–105. https://doi.org/10.1016/j.jaap.2011.04.010.
Wen, J.-L., Sun, S.-L., Yuan, T.-Q., Xu, F., Sun, R.-C., 2014. Understanding the chemical and structural transformations of lignin macromolecule during torrefaction. Appl. Energy 121, 1–9. https://doi.org/10.1016/j.apenergy.2014.02.001.
Widowati, W., Asnah, A., 2014. Biochar effect at potassium fertilizer and dosage leaching potassium for two-corn planting season. AGRIVITA J. Agric. Sci. 36 https://doi.org/10.17503/Agrivita-2014-36-1-p065-071.
Yan, J., Zuo, X., Yang, S., Chen, R., Cai, T., Ding, D., 2022. Evaluation of potassium ferrate activated biochar for the simultaneous adsorption of copper and sulfadiazine: competitive versus synergistic. J. Hazard Mater. 424, 127435 https://doi.org/10.1016/j.jhazmat.2021.127435.
Yu, J., Guo, Q., Gong, Y., Ding, L., Wang, J., Yu, G., 2021. A review of the effects of alkali and alkaline earth metal species on biomass gasification. Fuel Process. Technol. 214, 106723 https://doi.org/10.1016/j.fuproc.2021.106723.
Zhang, J., Shao, J., Jin, Q., Zhang, X., Yang, H., Chen, Y., Zhang, S., Chen, H., 2020a. Effect of deashing on activation process and lead adsorption capacities of sludge-based biochar. Sci. Total Environ. 716, 137016 https://doi.org/10.1016/j.scitotenv.2020.137016.
Zhang, S., Min, G., Wang, J., Zhu, S., Zhang, H., Liu, X., 2020b. Release characteristics of potassium and chlorine for torrefied wheat straw during a combined pyrolysis-combustion system. Bioresour. Technol. 312, 123591 https://doi.org/10.1016/j.biortech.2020.123591.
Zhang, S., Su, Y., Ding, K., Zhang, H., 2019. Impacts and release characteristics of K and Mg contained in rice husk during torrefaction process. Energy 186, 115888. https://doi.org/10.1016/j.energy.2019.115888.

Zhang, Z., Liu, J., Shen, F., Wang, Z., 2020c. Temporal release behavior of potassium during pyrolysis and gasification of sawdust particles. Renew. Energy 156, 98–106. https://doi.org/10.1016/j.renene.2020.04.076.
Zheng, A., Jiang, L., Zhao, Z., Huang, Z., Zhao, K., Wei, G., Wang, X., He, F., Li, H., 2015. Impact of torrefaction on the chemical structure and catalytic Fast pyrolysis behavior of hemicellulose, lignin, and cellulose. Energy Fuels 29, 8027–8034. https://doi.org/10.1021/acs.energyfuels.5b01765.
Zhu, L., Zhao, N., Tong, L., Lv, Y., 2018. Structural and adsorption characteristics of potassium carbonate activated biochar. RSC Adv. 8, 21012–21019. https://doi.org/10.1039/C8RA03335H.